

Heat Transfer and Friction in Rectangular Duct with Pin-Fin Arrays

C. Mageswaran¹ R.Muthukumar² R. Karthikeyan³ and R. Rathnasamy⁴

¹Research scholar²Assistant professor³Associate professor ⁴Professor,
Mechanical Engineering, Annamalai University,
Annamalainagar, Tamilnadu, 608002, India

Abstract: This study involves an experimental investigation of pin-fin heat sinks have circular, square and diamond cross-sections. Ensemble of pin-fin heat sinks with in-line and staggered arrangements were designed and tested. The fin density effect on heat transfer and friction characteristics is examined. The channel cross section is of 150 mm x 200 mm. The experiments covered the following ranges: Reynolds number 2000 to 25000, clearance ratio (C/H) 0.0 to 0.50 and inter-fin spacing ratio ($S_y/d=1.2$ to 22.8 and $S_x/d=1.2$ to 10). In all, the circular pin-fin arrangement shows an appreciable influence of fin density and whereas no effect is seen in case of square fin geometry. This is associated with the unique deflection flow pattern accompanied with the in-line circular fin configuration. For the staggered arrangement, the heat transfer coefficient increases with the rise of fin density with the penalty of pressure drop. However, diamond pin-fin results the lowest pressure drop with better performance than that square configuration.

Keywords: Clearance ratio, duct flow, forced convection, heat sink, pin-fin performance, pressure drop

1. INTRODUCTION

Rapid development in information technology allows portable electronics to gain faster processing speed and enhanced capabilities. However, thermal management in the portable electronics environment is becoming increasingly difficult due to high heat load and dimensional constraints. Increasing the heat transfer area is preferred as the simplest method to enhance heat dissipation rate, because the use of better fluid to increase the heat transfer coefficient is not an economical and practical solution. The one of the controllable variable to enhance the convective heat transfer rate from an extended surface is the geometry of the fins.

Attaching fins increases the surface area but it also increases the resistance to the flow of air. The heat transfer coefficients based on base area of the fin arrays may be less than that of the base plate. If the decrease in the heat transfer coefficient is more than the increase in the surface area, the heat transfer rate will decrease. The current trend in electronic industry is microminiaturization of electronic packages. The thermal design problem is recognized as one of the factors limiting achievement of higher packaging densities. Because of reduction in surface area available for heat dissipation, optimization of fin surface area and geometry becomes very important in natural and force convection heat transfer.

It is evident from the previous investigations (VanFossen, 1982, Metzger *et al.* 1984, Armstrong, J and Winstanely, D, 1988, Chyu 1990, Babus'Haq *et al.* 1995, Chyu *et al.* 1998, Tahat *et al.* 2000 and Sara 2003) pin-fin arrays dissipate higher heat transfer than plain channels and is always accompanied by a substantial increase in pressure loss. Therefore, in most applications of pin-fins, both the heat transfer and pressure loss characteristics must be considered. On the other hand, the pin-fins with various cross-sections have different heat transfer and flow resistance characteristics, though circular pin fins do perform the best. Therefore, it is essential to investigate pin fins of various cross-sections in order to enhance the heat transfer and decrease the flow resistance. It is the aim of this study to investigate the heat transfer, pressure and performance characteristics for the in-line and staggered pin-fin arrays (cylinder, square and diamond) attached on a flat surface in a rectangular channel by considering various geometric and flow parameters.

2.0 EXPERIMENTAL SET-UP

The various components involved in the set-up are given below.

2.1 Pin-fin assembly

The pin-fin arrays considered for this investigation are having circular ($d=10$ mm $H=90$ mm), square and diamond (fin-size 9.2×9.2 mm² of height (H) 7.68 mm) cross-section and are protruding vertically upwards from a 250 mm x 145 mm horizontal rectangular base having thickness 25.4 mm as shown in Fig.1. The maximum and minimum numbers of pin-fins used in this investigation are 220 and 22 respectively. Spacing is varied from 12 to 120 mm in the span-wise direction and from 12 to 228 mm in the stream-wise direction. The rectangular base as well as the pin-fins was manufactured from a light aluminum alloy (i.e.; duralumin). For each test, the pin-fin height was kept constant with clearance(C) zero and 0.5 H between the tips of the pin-fins and the shroud (adjustable roof).

2.2 Wind-tunnel

A rectangular cross-sectioned wind-tunnel duct was manufactured from 19 mm thick plywood and about 2 m long with a constant internal width of 150 mm. Fig.2 shows the schematic of the experimental set-up. A bell-mouth section was fitted at the entrance of the wind-tunnel duct followed by a low porosity, cardboard honeycomb flow-straightner. The heated air from the pin-fin assembly

was passed through an insulated chamber, where mixing was accomplished by two cardboard honeycombs mounted perpendicular to the flow-stream, one being of relatively low porosity and the other of higher porosity. The latter was situated upstream of the former. At the exhaust end of the duct, a gradual area-contraction section attached is used to connect a single-speed, single-stage blower (via G.I. pipe). Blower was capable of providing a maximum flow rate of 0.242 kg/s, and is preceded by a butterfly throttle control valve. A differential manometer was employed to measure the pressure drop across calibrated orifice plate (see Fig.) to indicate mass-flow rate of air. The wind tunnel was operated in the suction mode, i.e.; the blower sucked atmospheric air via the bell-mouthed entrance section that flow over pin-fin assembly of the test section. This avoids the air-stream being heated by the blower during compression/friction prior to its travel to the heat-exchanger assembly and enhanced the cooling capability of the air. A plate electric heater consisting of nichrome wire wound on a mica sheet and covered on either side with another mica sheet and electric connections are also provided appropriately to supply power for heating. It has a capability to deliver 1500 W. The heat exchanger base was heated uniformly to maintain constant temperature. A horizontal guard heater, rated at 500 W, was positioned, parallel to the main heater. The whole heat-exchanger base, main heater and guard heater, with associated thermal insulations, was located in and protected in a well-fitted

open-top wooden box. The horizontal upper edges of this box and the top surfaces of the laterally-placed thermal insulant are leveled in order to have smooth flow with the upper surface of the rectangular base where the fins protrude upwards.

2.3 Heating system

The steady-state temperatures at the base of the pin-fin array are measured by a set of nine copper-constantan (T-type) thermocouples embedded and appropriately distributed within the rectangular base. The base plate was thick enough to maintain uniform temperature of 50°C rather than uniform heat flux achieved normally employing a thin plate. The inlet and the outlet air-stream temperatures in the wind-tunnel duct were measured using eight thermocouples and 6 RTDs. Each experiment is continued for half an hour after steady-state conditions were attained.

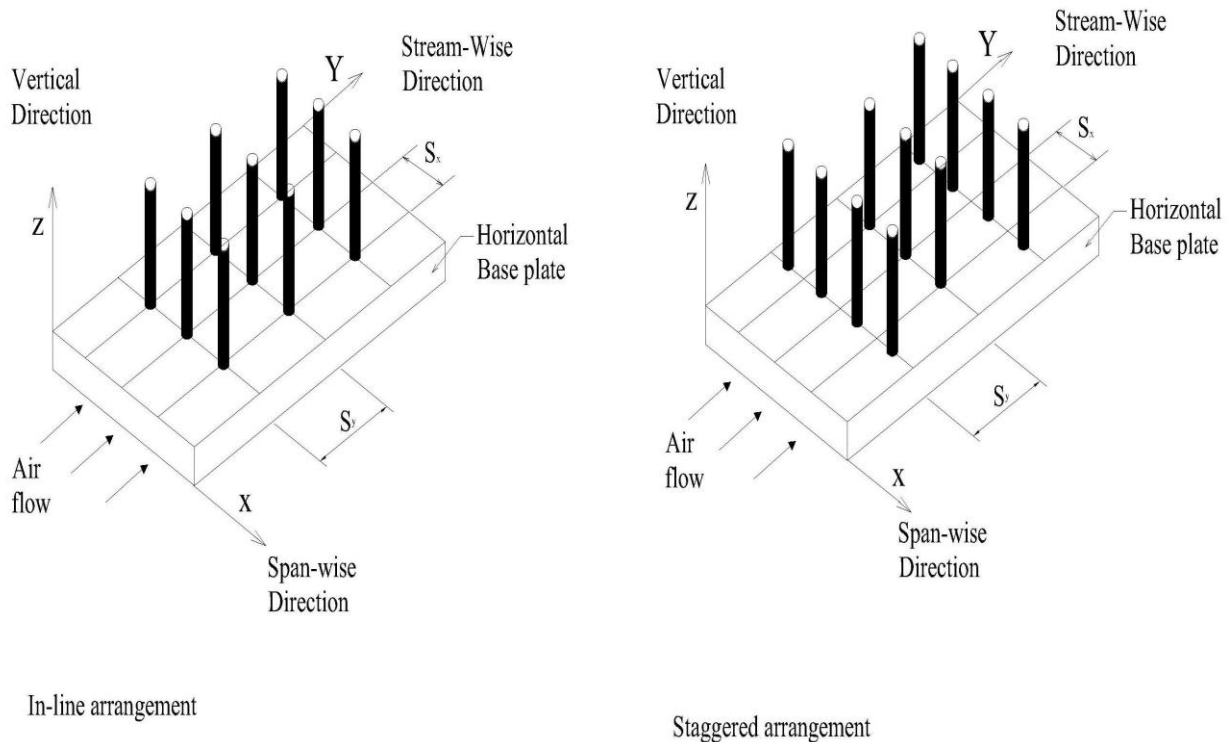


Fig. 1 Pin-fin assembly

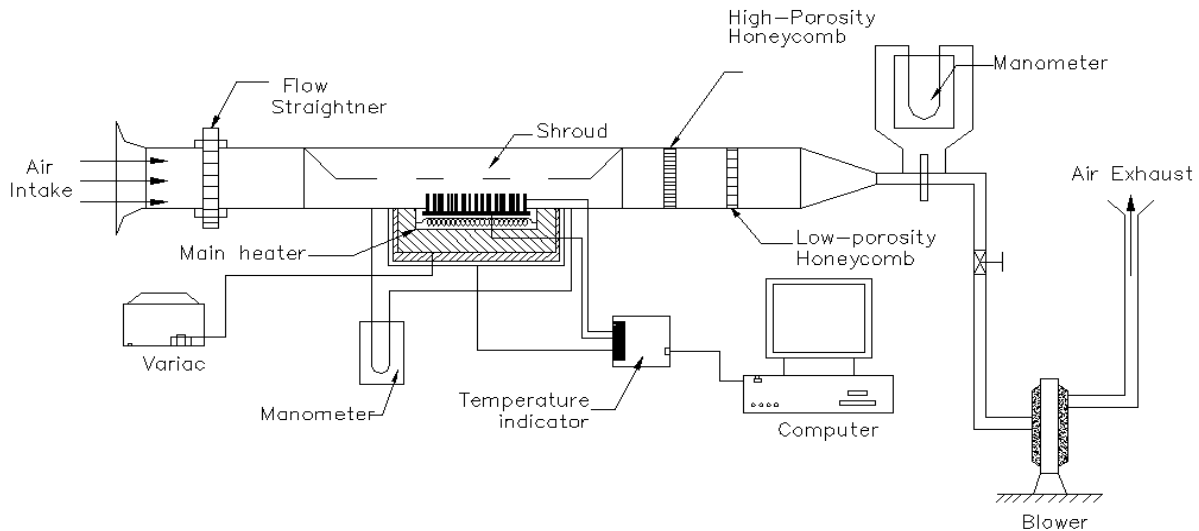


Fig.2 Schematic of the experimental set-up

3.0 DATA REDUCTION

The data generated during the various trials are used to evaluate the heat transfer and friction characteristics. The steady state heat transfer from the finned surface is,

$$Q_{tot} = Q_{conv} + Q_{rad} + Q_{loss} \quad (1)$$

In the present study the data reduction is similar to that followed by Tahat *et al.* (2000) and Sara (2003). They conducted experiments and fin arrays are comparable and reported that the total heat loss from the assembly ensue less than 5%. Under the present operating conditions together with the fact that the test section is well insulated and assuming the loss is very minimum, eqn. (1) is rewritten as,

$$Q_{conv} = mc_p (t_{out} - t_{in}) \quad (2)$$

The heat transfer by convection from fin surface including base plate is given by,

$$Q_{conv} = h A_s \left[t_b - \left(\frac{t_{in} + t_{out}}{2} \right) \right] \quad (3)$$

where, t_{in} and t_{out} are the temperatures of air flow, t_b is the average temperature at certain designated locations on the base assembly and A_s is the total surface area of base assembly and fins, which is given as,

$$A_s = WL + \pi d H N_{xy} - \frac{\pi d^2 N_{xy}}{4} \quad (4)$$

The average heat transfer coefficient for the heated pin-fin assembly can be calculated by combining eqns. (2) and (3) under the present operating conditions together with the fact that the test section was well insulated.

$$h = \frac{m c_p (t_{out} - t_{in})}{A_s \left[t_b - \left(\frac{t_{in} + t_{out}}{2} \right) \right]} \quad (5)$$

The free flow area A_{ff} is calculated as,

$$A_{ff} = W(H + C) - N_x H d \quad (6)$$

The Reynolds number (Re) is defined in the conventional way as,

$$Re = \frac{G d}{\mu} \quad (7)$$

where, $G = m/A_{ff}$ is the mass flux.

4.0 RESULTS AND DISCUSSIONS

The various heat transfer associated parameters evaluated above are used to analyse the influence on heat transfer with pin-fin. The obtained results for individual parametric influence on heat transfer are discussed in separate or combined; i) pin-fin spacing and area (number of fins), ii) pin-fin shape (cross-section) and iii) pin-fin array.

4.1 Effect of pin-fin spacing

Heat transfer measurements were carried out by varying $S_x=12$ to 120 mm and $S_y=12$ to 228 mm with two values of C/H , namely; 0.0 and 0.5. In each case, measurements were obtained for six values of mass flow rates, namely; 0.069, 0.089, 0.105, 0.119, 0.132 and 0.143 kg/s and correspondingly the Reynolds number used in experiment ranges from 2000 to 25000. Under these specified values of C/H and air flow rates and for the in-line arrangement, plots of Nusselt number *versus* stream-wise spacing ratio (S_y/d) is depicted in Fig.3. From the plots, it is clearly seen that an increase in mass flow rate and spacing improves the performance of the pin-fin array. However, Nusselt number is increasing as the value of S_y or S_y/d increases and decreases after certain values of S_y . It

is presumed that there is an optimum value of S_y for maximum Nusselt number. Therefore in order to identify the optimum spacing the fig. 3 is re-plotted along with second order polynomial fit as shown in fig.4. However, optimum point is not clearly seen in the covered range of spacing to take as the optimum spacing for the array. The optimum value of S_y could lie between two vertical lines as marked in the plot. Fig.5 depicts spacing effect for square in analogous to cylinder.

Correspondingly, a plot of Nusselt number *versus* span-wise spacing ratio (S_x/d) is shown in fig.6 for cylinder. The behaviour of the pin-fin for variation in S_x is similar to that of variation in S_y . Here again it is presumed for optimum values of S_x to lie between $S_x = 20$ to 30 mm.

4.2 Effect of pin-fin shape and array

The heat transfer enhancement in pin-fin array is achieved by introducing turbulence (flow re-attachment or delay separation). Fig.7 shows the pin-fin profile shape (cylinder, square and diamond) influence on heat transfer enhancement. Despite that the foretold three pin-fin profile have unique surface area, the diamond fins perform better than cylinder and square as well. Among these staggered pin-fin arrays show better performance than the other configuration. This is in view of the fact that wake flow effect is less pronounced after the first row pin-fins. The free flow fluid/air between any two adjacent pin-fins of the upstream row is subject to flow over the subsequent down stream rows and hence introduces fresh boundary layer growth that promotes heat transport mechanism. For staggered array, the path of the main flow is more tortuous/convoluted (i.e; increases the flow path length or fluid residence time). A greater portion of the surface area of the down stream pin-fins remained in the flow path (Incropera and DeWitt 1990) and enhanced the heat transfer compared to that for the in-line array performance.

5.3 Effect of fin number and flow rate on pressure drop

It is not uncommon that the flow resistance is an important aspect in heat transfer in order to have minimum pumping power as a constraint. The variation of pressure drop for various flow rates as plot of friction factor *versus* Reynolds number is illustrated in fig.8 for $C/H=0.0$. In the case of cylinder it is clear that increase in packing density (N_{xy}) influence the friction factor increase as seen from fig. 8. A similar plot is shown in fig.9 for cylinder and square module.

In fig.9 it is observed that there is only little variation in friction resistance between cylinder and square for same configuration. Given the configuration of pin-fin the staggered array exhibit higher pressure drops or pumping power and it is also seen in fig.10 shown. This can be attributed to the fact that staggered arrangement restricts working fluid easily flowing between the fins as in the case of in-line array, blockading the channel like passage of the fluid between the fins.

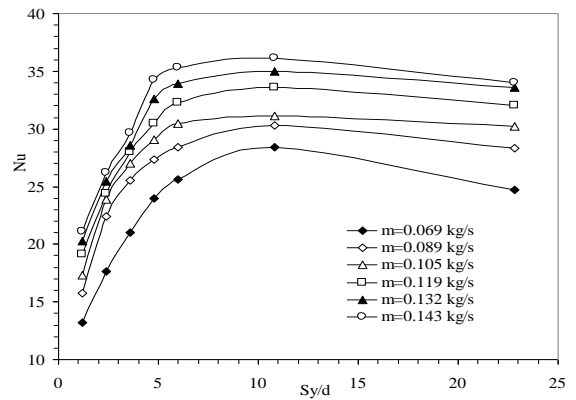


Fig. 3 Plot of Nusselt number vs S_y/d for $C/H=0$, $S_x= 12$ (cylinder)

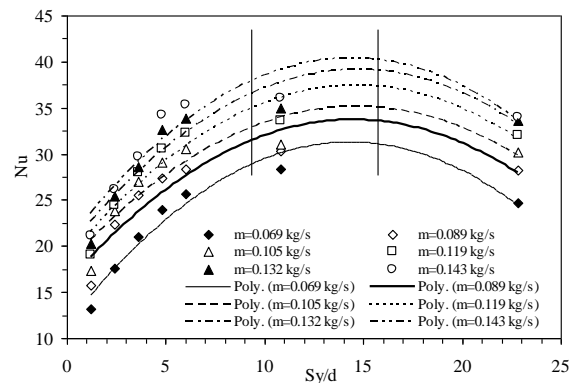


Fig. 4. Plot of Nusselt number vs S_y/d for $C/H=0.0$, $S_x= 12$ (cylinder)

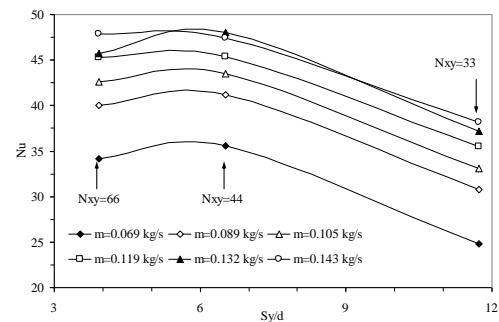


Fig. 5 Plot of Nusselt number vs S_y/d for $C/H=0$, $S_x= 12$ (square)

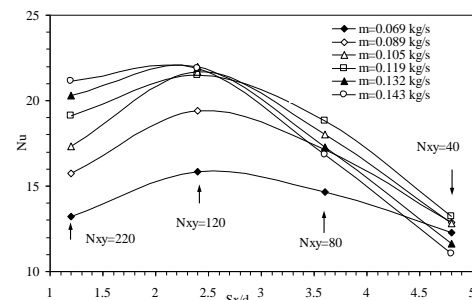


Fig. 6 Plot of Nusselt number vs S_x/d for $C/H=0$, $S_y= 12$ (cylinder)

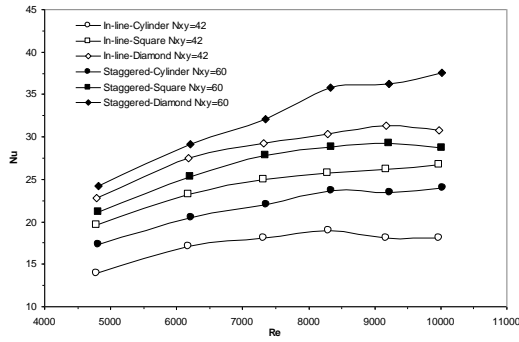


Fig. 7 Effect of pin-fin-shape on Nu for C/H=0, $S_x=24$, $S_y=24,36$

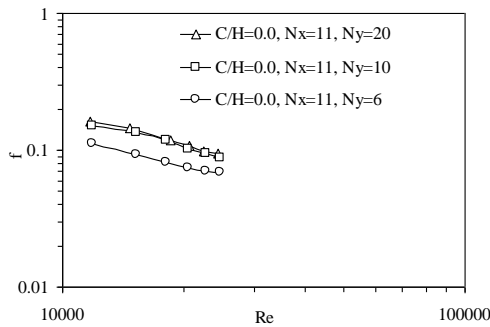


Fig. 8 Plot of 'f' vs Reynolds number $S_y= 12, 24$ and 36 mm (cylinder)

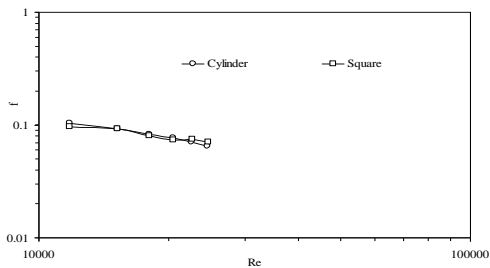


Fig. 9 Plot of 'f' vs Reynolds number for $C/H=0$, $N_{xy}=77$; $S_x=12$, $S_y=36$

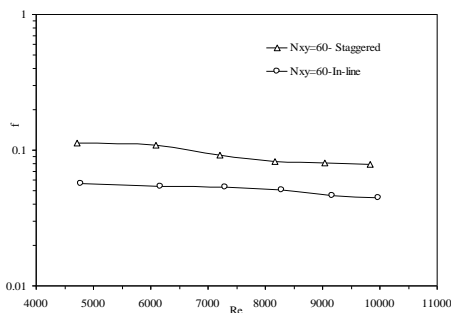


Fig. 10 Plot of 'f' vs Reynolds number for $C/H=0$, $S_x=24$ $S_y=24$.

6.0 CONCLUSIONS

The conclusions arrived from present study are

- i) The variation in spacing on both span-wise and stream-wise directions have effect on Nusselt number.

- ii) The change in Nusselt number is more rapid for stream-wise direction (S_y) than that for the span-wise direction (S_x).
- iii) For a given Reynolds number, the pin-fin array with particular inter-fin distance or number of pin-fins gives higher performance than those at other values
- iv) The staggered array produce slightly higher enhancement than the in-line arrangement. However, as a consequence of the heat transfer enhancement the pressure drop was higher.
- v) As for pin-fin shape is concerned, the diamond fins perform better heat transport than cylinder and square as well: even though cylinder, square and diamond have unique fin surface area.
- vi) There is a little variation in the friction factor between cylinder and square with same configuration and staggered arrangement has more friction than the in-line counterpart.

Nomenclature

A	area, m^2
C	clearance between fin tip and the roof, mm
C_p	specific heat of air, J/kg K
d	diameter of the pin-fin, mm
f	friction factor
G	mass flux, $kg/m^2 s$
H	height of the pin-fin, mm
k	thermal conductivity, W/m K
L	length of the base plate, mm
m	mass flow rate of air, kg/s
N	number of pin-fin
Nu	Nusselt number
Q	heat transfer rate, W
Re	Reynolds number
S	spacing, mm
t	temperature, $^{\circ}C$
T	temperature, K
W	width of the base plate, mm
x, y, z	set of Cartesian coordinates
Δp	overall pressure drop along the array, N/m^2
μ	dynamic viscosity, $N s/m^2$
ρ	density, kg/m^3

Subscripts

a	air
b	base plate
conv	convection
ff	free flow
in	inlet condition
loss	loss of heat
out	outlet condition
rad	radiation
tot	total
ts	total surface
x, y	directions

REFERENCES

- [1] Armstrong, J. and Winstanley, D. 1988 A review of staggered array pin-fin heat transfer for turbine cooling applications. *J. Turbomachinery*, 110, 94-103
- [2] Babus'Haq, R.F., Akintunde, K. and Probert, S.D. 1995 Thermal performances of a pin fin assembly. *Int. J. Heat & Fluid Flow* 16, 50-55
- [3] Chyu, M.K. 1990 Heat transfer and pressure drop for short pin-fin arrays with pin-endwall fillet. *J. Heat Transfer ASME*, 112, 926-932.
- [4] Incropera F.P. and De Witt D.P. 1985 *Fundamentals of heat and mass transfer*, 2nd Edition. New York: John Wiley.
- [5] Jurban, B.A., Hamdan, M.A. and Abdualh, R.M. 1993 Enhanced heat transfer, missing pin and optimization for cylindrical pin-fin arrays. *J. Heat Transfer*, 115, 576-583.
- [6] Sara, O.N. 2003 Performance analysis of rectangular ducts with staggered square pin fins. *Energy Conservation and Management*, 44, 1787-1803.
- [7] Tahat, M., Kodah, Z.H., Jarrah, B.A. and Probert, S.D. 2000 Heat transfer from pin-fin arrays experiencing forced convection. *Applied Energy*, 67, 419-442.
- [8] VanFossen, G.J. 1982 Heat transfer coefficients for staggered arrays of short pin-fins, *ASME J. of Eng. for Power*, 104, 268-274.